Applied Magnetic Resonance
https://doi.org/10.1007/s00723-025-01785-w

Applied
Magnetic Resonance

ORIGINAL PAPER

Proton MRD Profile Analysis in Human Serum Albumin Solutions: Two and Three Sites Exchange Model Approaches

Néstor Juan Rodríguez de la Cruz[1] · Carlos Alberto Cabal Mirabal[2,3] · Robert N. Müller[4] · Sophie Laurent[4] · Fabian Tamayo Delgado[2] · Juan Carlos García Naranjo[2] · Yasser Rodríguez de la Cruz[1] · Manuel Arsenio Lores Guevara[2,3]

Received: 23 May 2025 / Revised: 19 July 2025 / Accepted: 30 July 2025

Abstract

The two sites water exchange model (2SWEM) and the three sites exchange model (3SEM) were properly used to describe proton (^{1}H) magnetic relaxation dispersion (^{1}HMRD) in human serum albumin (HSA) solutions at 310 K. Lyophilized HSA was obtained from Sigma-Aldrich and diluted in phosphate buffered saline (PBS, pH 7.4) to obtain 10 samples with a concentration of 50 g/l. The ^{1}HMRD profiles (20–60 MHz) were obtained using a fast field cycling nuclear magnetic resonance relaxometry facility (Stelar FFC 2000 Spinmaster) and two Minispec (Mq20, Mq60) relaxometry facilities from Bruker. The longitudinal ^{1}H magnetic relaxation time (T_1) was measured employing the inversion recovery pulse sequence and the $1/T_1$ was plotted as a function of the frequency of resonance to create the ^{1}HMRD profiles. The 2 sites water exchange model considering ellipsoidal geometry is the best option to fit the ^{1}HMRD profiles in diluted HSA solutions, which allows to update the physical model previously presented to describe the theoretical dependence between the transverse proton magnetic relaxation rate and the protein dynamic viscosity in blood plasma and blood serum solutions. The physical parameters obtained from the fit, using this model, describe properly the diluted HSA solutions in comparison with previous experimental reports and theoretical estimations. This result can be improved taking into consideration all the proton–proton dipolar interactions of the protons belonging to the bound water molecules.

Keywords ^{1}HMRD profiles · HSA · Two sites water exchange model · Three sites exchange model

Extended author information available on the last page of the article

Published online: 11 August 2025

1 Introduction

Proton (^{1}H) magnetic relaxation (PMR) studies of protein solutions have been successfully used to develop medical applications [1–8]. The behaviors of the transverse (T_2) and longitudinal (T_1) proton magnetic relaxation times in intracellular hemoglobin (Hb) solutions have allowed to determine the delay time of the hemoglobin S (HbS) polymerization process [1, 2, 7] in sickle cell disease (SCD) [9–14], giving the possibility of to differentiate the crisis and the steady state in SCD patients [1, 2, 7], as well as to evaluate a potential treatment [1, 2, 7, 15–17]. On the other hand, the values of T_2 have been employed to determine the dynamic viscosity (η) of Hb [4, 6], blood plasma [5], blood serum [3] and whole blood [17]. To improve these medical applications, or to create new applications, a proper understanding of PMR in protein solutions is needed.

The method based on PMR to evaluate η in blood plasma samples has been very useful during the clinical evaluation of patients with SCD and Multiple Myeloma [5] and also to determine the blood dynamic viscosity [17]. Considering that human serum albumin (HSA) is the main content in blood plasma, a proper description of PMR in solutions of HSA is needed, especially in experimental conditions near to the physiological conditions (50 g/l and 310 K).

Different models have been considered to describe PMR in protein solutions from the seminal paper of Dazkiewic in 1963 until now [1, 3, 5, 6, 15, 18–31]. Koenig and coworkers [23, 24, 28] developed three mathematical equations to fit the nuclear magnetic relaxation dispersion (NMRD) profiles, which are not completely based (or not based) in the theory of PMR. Despite this fact, the Hallenga and Koenig approach [28] is often used to fit the NMRD profiles. The most widely used physical model to describe PMR in protein solutions is the 2 sites water exchange model (2SWEM) [18–25, 27], see appendix:

$$R_1(\omega_0) = R_{1w}^{\text{bulk}} + \delta_1 \left[\frac{0.2\tau_{\text{R}}}{1+\omega_0^2\tau_{\text{R}}^2} + \frac{0.8\tau_{\text{R}}}{1+4\omega_0^2\tau_{\text{R}}^2} \right]$$

$$\delta_1 = P_B \frac{3}{2} \left(\frac{\mu_0}{4\pi} \right)^2 \left(\frac{\gamma^4 \hbar^2}{b^6} \right) \tag{1}$$

In Eq. (1), R_1 is the longitudinal proton magnetic relaxation rate due to the presence of the protein in the aqueous solution and R_{1w}^{bulk} is the contribution to the relaxation rate from the solvent alone. P_B is the fraction of water bound (B) to the protein, μ_0 is the magnetic permeability of the vacuum, $\hbar$ is the Planck's constant divided by 2π, γ is the magnetogyric ratio of the ^{1}H and $b = 1.5810^{-10}m$ is the distance between the protons inside the water molecule. On the other hand, ω_0 is the angular frequency of resonance and τ_R is the rotational correlation time of the protein molecule. Here, the water molecules are considered irrotationally bound to the macromolecule and the dipolar interaction between the protons inside the water molecule is assumed as the main contribution to PMR [3, 5, 6, 18, 19]. In this case the interacting spin pairs (protons inside the water molecule irrotationally bound to the

protein) are embedded in one rigid molecule with spherical geometry and rotating with just one correlation time: τ_R (see appendix).

Another approach to describe PMR in protein solutions is the three sites exchange model (3SEM) [18, 29, 31]. In addition to the water in the solvent (characterized by a fraction of water P_{Bulk}), in this model two types of water bound to the protein are considered: the water irrotationally bound (B^*) to the protein or internal water (characterized by a fraction of water P_B^*) and the water bound to the surface of the macromolecule, but free to rotate at its binding site, or hydrated water (hy), which is characterized by a fraction of water P_{hy}($P_{Bulk} + P_B^* + P_{hy} = 1$). A fast exchange of water molecules is established among these 3 sites for the water molecules [18, 29, 31] and we can write for R_1:

$$R_1(\omega_0) = R_{1w}^{\text{bulk}} + \alpha + \delta_1^* \left[\frac{0.2\tau_{\text{R}}}{1 + \omega_0^2\tau_{\text{R}}^2} + \frac{0.8\tau_{\text{R}}}{1 + 4\omega_0^2\tau_{\text{R}}^2} \right] \tag{2}$$

In Eq. (2), $\alpha = P_{hy}R_1^{hy}$, being R_1^{hy} the magnetic relaxation rate of the protons belonging to the hydrated water, and δ_1^* is defined as δ_1 but changing, in Eq. (1), P_B by P_B^*, such as $P_B = P_B^* + P_{hy}$.

Despite Eqs. (1) and (2) are the traditional models to describe PMR in protein solutions, frequently the geometry of the protein is more near to one ellipsoid than to one sphere (mainly in solution) [32–35]. This is the case of the solutions of HSA, where the protein is described as a prolate ellipsoid with lengths of $140{\cdot}10^{-10}$ m for its major axis and $40{\cdot}10^{-10}$ m for its minor axis [34, 35]. Here, the option is to consider the interacting spin pairs as embedded in one rigid molecule with ellipsoidal geometry and rotating with more than one correlation time. Then, Eqs. (1) and (2) can be rewritten as follows (see appendix):

$$R_1(\omega_0) = R_{1w}^{\text{bulk}} + \sum_{i=1}^{2} \beta_i \left[\frac{0.2\tau_{\text{Ri}}}{1 + \omega_0^2\tau_{\text{Ri}}^2} + \frac{0.8\tau_{\text{Ri}}}{1 + 4\omega_0^2\tau_{\text{Ri}}^2} \right] \tag{3}$$

$$R_1(\omega_0) = R_{1w}^{\text{bulk}} + \alpha + \sum_{i=1}^{2} \beta_i^* \left[\frac{0.2\tau_{\text{Ri}}}{1 + \omega_0^2\tau_{\text{Ri}}^2} + \frac{0.8\tau_{\text{Ri}}}{1 + 4\omega_0^2\tau_{\text{Ri}}^2} \right] \tag{4}$$

In Eq. (3), β_1 and β_2 are the magnitudes of the dispersions associated with two different rotations of the ellipsoidal protein: the first one around one axis parallel to the main symmetry axis of the ellipsoid and the second one around one axis perpendicular to this main symmetry axis (see appendix). On the other hand, τ_{R1} and τ_{R2} are the rotational correlations times associated with these two rotations. In Eq. (4), β_1^* and $\beta_2^*$are defined as β_1 and β_2 (see appendix) but changing δ_1 by δ_1^*.

In this work we have focused in the analysis of the proton magnetic relaxation dispersion (^{1}HMRD) profiles, measured in solutions of HSA of 50 g/l and at 310 K, to define which is the best physical model (between the 2SWEM and the 3SEM) to describe PMR in these solutions. Considering the geometry of the HSA in solutions we have used an ellipsoidal geometry to compare the performances of the 2SWEM

and the 3 SEM. Taking into account the traditional approach used to describe PMR in protein solutions, these results were compared with the performances of both models considering spherical geometry.

2 Materials and Methods

Lyophilized HSA was obtained from Sigma-Aldrich and diluted in phosphate buffered saline (PBS, pH 7.4) to obtain 10 samples with a concentration of 50 g/l; 500 µl of protein solution were transferred to a NMR tube for the measurements.

A fast field cycling nuclear magnetic resonance relaxometry facility (Stelar FFC 2000 Spinmaster) was used, in the range from 20 kHz to 10 MHz, to obtain the longitudinal ^{1}HMRD profiles at 310 K, which were represented as semilog plots of R_1 ($1/T_1$) versus $f_0 = \omega_0/2\pi$. Additional points at 20 MHz and 60 MHz were added after measuring the samples in the Mq20 and Mq60 relaxometry analyzers (Minispec) from Bruker. For each sample at least five ^{1}HMRD profiles were measured (to obtain a total of 50 ^{1}HMRD profiles measured for HSA samples of 50 g/l) and the values of the obtained parameters reported as: $\overline{u} \pm \mathrm{SD}$. Here, $\overline{u}$ and SD represent the mean value and the standard deviation of the performed measurements, respectively. A Student's test (t test) was used to compare means with $\alpha = 0.05$.

During the fitting of the experimental ^{1}HMRD profiles to the 2SWEM and the 3SEM, using ellipsoidal geometry, the values of R_{1w}^{bulk} were fixed to avoid overfitting and the values of α were taken such as $\alpha \geq 0$ to avoid unphysical (negative) results.

3 Results and Discussion

Figures 1 and 2 show the typical ^{1}HMRD profile obtained in HSA solutions (50 g/l) at 310 K. In Fig. 1, the ^{1}HMRD profile was fitted using Eqs. (1) and (2) corresponding to the 2SWEM and the 3SEM, respectively, considering a spherical geometry for the HSA. In Fig. 2, the ^{1}HMRD profile was fitted using Eqs. (3) and (4) corresponding to the 2SWEM and the 3SEM, respectively, considering an ellipsoidal geometry for the HSA. The parameters resulting from the fit of the experimental ^{1}HMRD profiles using Eqs. (1)–(4) appear summarized in Table 1.

Experimental evaluations of R_1 in pure water performed during this study showed a value of 0.33 s^{-1} (310 K), which is significantly lower than our values of R_{1w}^{bulk} (around 0.40 s^{-1}, see Table 1). Considering that our samples of HSA solutions are extremely diluted saline solutions (lyophilized HSA was diluted in PBS until reach 50 g/l), T_1 values will decrease as a consequence of the saline content and the $R_1 = 1/T_1$ will increase. T_1 and R_1 will slightly change due to the concentration of salts is really small in PBS. The values of R_{1w}^{bulk} obtained using the two models (2SWEM and 3SEM) and the two geometries for the HSA molecule (spherical and ellipsoidal geometries) are coincident (see Table 1).

The values of τ_R, τ_{R1} and τ_{R2} obtained in this work (see Table 1) correspond with the range of values reported in the literature for the rotational correlation

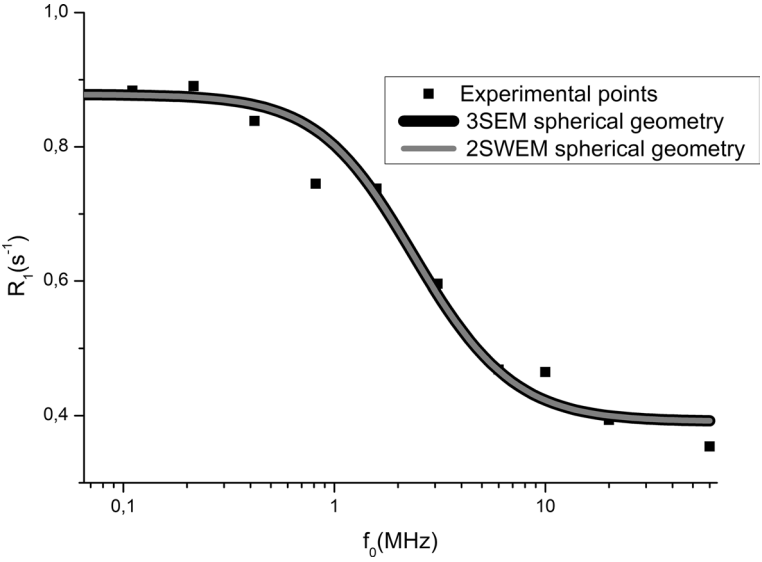

Fig. 1 Typical ^{1}HMRD profile in HSA solutions of 50 g/l at 310 K. The profile has been fitted using the 2SWEM and the 3SEM considering spherical geometry for the HSA. The fits obtained overlaps

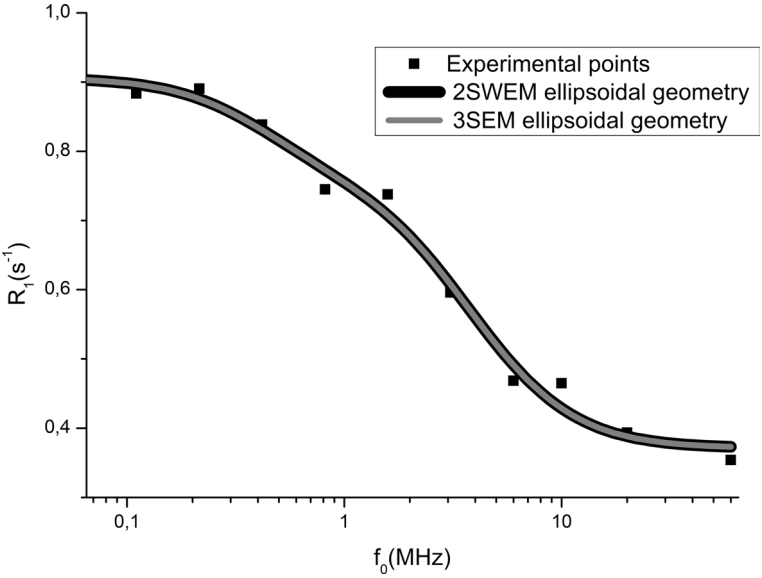

Fig. 2 Typical ^{1}HMRD profile in HSA solutions of 50 g/l at 310 K. The profile has been fitted using the 2SWEM and the 3SEM considering ellipsoidal geometry for the HSA. The fits obtained overlaps

Table 1 Values of the proton magnetic relaxation rate of the solvent (R_{1w}^{bulk}); the rotational correlation time for the movement of the HSA molecule considered as one sphere (τ_R), the magnitudes of the dispersion for the 2SWEM (δ_1) and the 3SEM (δ_1^*) considering spherical geometry for the macromolecule, the proton magnetic relaxation rate for the hydrated water (α), the magnitudes of the dispersions for the 2SWEM (β_1 and β_2) and the 3SEM (β_1^* and β_2^*) considering ellipsoidal geometry for the HSA molecule and the rotational correlation times for the movement of the HSA as one ellipsoid (τ_{R1} and τ_{R2}). These parameters were obtained from the fit of the experimental ^{1}HMRD profiles (310 K, 5 profiles per sample) to the 2SWEM and the 3SEM in 10 samples of HSA (50 g/l) considering spherical and ellipsoidal geometries for the protein. $\overline{R}^2$ is the adjusted value of the coefficient of determination (R-square)

Parameters	2SWEM Sphere	2SWEM Ellipsoid	3SEM Sphere	3SEM Ellipsoid
$R_{1w}^{bulk}(s^{-1})$	0.405 ± 0.021	0.378 ± 0.011	0.400 ± 0.013	0.400 ± 0.024
$\delta_1 \times 10^7$ (s^{-2})	1.180 ± 0.161			
$\delta_1^* \times 10^7$ (s^{-2})			1.226 ± 0.147	
$\tau_R \times 10^{-8}$ (s)	4.180 ± 0.429		4.158 ± 0.492	
$\alpha \times 10^{-4}$ (s^{-1})			0.032 ± 0.007	0.047 ± 0.028
$\beta_1 \times 10^7$ (s^{-2})		1.384 ± 0.190		
$\beta_1^* \times 10^7$ (s^{-2})				1.331 ± 0.155
$\tau_{R1} \times 10^{-8}$ (s)		2.739 ± 0.308		2.828 ± 0.243
$\beta_2 \times 10^5$ (s^{-2})		6.525 ± 1.763		
$\beta_2^* \times 10^5$ (s^{-2})				6.214 ± 1.779
$\tau_{R2} \times 10^{-7}$ (s)		2.349 ± 0.521		2.430 ± 0.540
$\overline{R}^2$	0.960 ± 0.010	0.977 ± 0.005	0.963 ± 0.011	0.976 ± 0.005

times of different proteins: (10^{-9}–10^{-7}) s [1, 2, 7, 18, 22–31], which has been widely established during the last 60 years using different experimental methods. For instance, Lindstrom and Koenig [24] reported in 1974, using NMRD, values between $9.5{\cdot}10^{-8}$ s and $2{\cdot}10^{-7}$ s for carbonmonoxihemoglobin (HbCO) depending on pH, concentration and temperature values. Hallenga and Koenig [28] reported in 1976 values between $4{\cdot}10^{-8}$ s and $4{\cdot}10^{-7}$ s for different proteins (Hemoglobin, Concanavalin A, Carbonic Anhydrase B, Lysozyme) and different values of temperature employing NMRD, Fluorescence Depolarization, Light Scattering and Dielectric Relaxation. Halle and coworkers [36] reported in 1981 values around 10^{-9} s for lysosyme, hemoglobin and human plasma albumin. K. Venu and coworkers [29] reported in 1997 values of the order of (5–7) 10^{-8} s for bovine pancreatic tripsin inhibitor (BPTI) at 300 K, pH 5.1 and 16.7 mM using NMRD. Kiihne and Bryant [25] reported in 2000 values between $4{\cdot}10^{-8}$ s and $5{\cdot}10^{-8}$ s for bovine serum albumin (BSA) employing NMRD. Lores and coworkers reported values for hemoglobin between 10^{-8} s and 10^{-7} s using Electronic Paramagnetic Resonance in 2006 [37] and NMRD in 2022 [18]. Moreover, Rodríguez and coworkers [6] estimated theoretically values of τ_R of the order of 10^{-7} s for hemoglobin in 2025. Finally, from special interest is that Olszewski reported in 1992 values from HSA, at 277 K and pH = 7.3, between $5{\cdot}10^{-7}$ s and $9{\cdot}10^{-7}$ s. This result is coherent with our experimental values of τ_R, τ_{R1} and τ_{R2} (Table 1) considering the correlation times depend exponentially of temperature and the argument of this exponential function depends on $1/T$, where T is the absolute temperature.

The rotational correlation times of the HSA depend of the geometry and dimensions of the rotating protein, as well as of the dynamic viscosity of the macromolecular solution (η_{HSA}), according to [38]

$$\tau_R^{pp} = \frac{32\pi a_1^3 S_1}{18kT}\eta_{HSA} \tag{5}$$

$$\tau_R^{pll} = \frac{32\pi a_1^3 S_2}{18kT}\eta_{HSA} \tag{6}$$

$$S_1 = \frac{\left(1-q^4\right)}{\left[\left(2-q^2\right)a_1 S^* - 2\right]} \tag{7}$$

$$S_2 = \frac{q^2\left(1-q^2\right)}{\left(2-q^2 a_1 S^*\right)} \tag{8}$$

$$S^* = 2\left(a_1^2 - a_2^2\right)^{\frac{-1}{2}} ln\left\{\left[a_1 + \left(a_1^2 - a_2^2\right)^{\frac{1}{2}}\right]/a_2\right\} \tag{9}$$

Here we have considered that the geometry of the HSA in solution is a prolate ellipsoid [34, 35]. τ_R^{pp} is the correlation time for the rotation around one axis perpendicular to the main axis of symmetry of the ellipsoid and τ_R^{pll} is the correlation time for the rotation around one axis parallel to this main axis of symmetry. On the other hand, a_1 and a_2 are the major and minor semiaxes of the HSA molecule, respectively, and $q = \frac{a_2}{a_1}$. In Eqs. (5) and (6), k is the constant of Boltzmann.

Considering that $a_1 = 70{\cdot}10^{-10}$ m and $a_2 = 20{\cdot}10^{-10}$ m [34, 35], and using Eqs. (5)–(9), the values of τ_R^{pp} and τ_R^{pll} for HSA, using similar concentration (46.7 g/l) and temperature (308 K) to those used in our experiment (50 g/l and 310 K), can be calculated as $7.4{\cdot}10^{-8}$ s and $1.91{\cdot}10^{-8}$ s, respectively, employing 0.95 mPa s for the η_{HSA} [34]. From Table 1, it is possible to see that the experimental values of τ_{R1} and τ_{R2}, obtained from the fit of the ^{1}HMRD profiles to the 2SWEM and the 3SEM considering ellipsoidal geometry, are near to the theoretically estimated values of τ_R^{pp} and τ_R^{pll}, particularly τ_{R1} from τ_R^{pll}.

The fits obtained with the 2SWEM and the 3SEM overlap for spherical and ellipsoidal geometries (see Figs. 1 and 2) because of the values of α (see Table 1) are much lower than the values of the other two terms at the right-hand side of Eqs. (2) and (4), and then α can be discarded in these equations making both models coincident. It can be supported considering the statistical coincidence between the values of τ_R, τ_{R1} and τ_{R2} obtained with the 2SWEM and the values of the same parameters obtained with the 3SEM (see Table 1). Moreover, the statistical coincidence between δ_1 and δ_1^* (Table 1) means, according to Eq. (1), that $P_B = P_B^*$; and, as $P_B = P_B^* + P_{hy}$ and $\alpha = P_{hy}R_1^{hy}$, then $P_{hy} = 0$ and $\alpha = 0$. In addition, the statistical coincidence

between δ_1 and δ_1^* provokes that $\beta_1 = \beta_1^*$ and $\beta_2 = \beta_2^*$ as can be observed in Table 1. From this analysis it is possible to conclude that the 2SWEM is enough to describe PMR in HSA solutions for the experimental conditions used in this work. It means that it is not necessary to split the bound water in two populations of water with different strengths in its binding to the macromolecule, it is enough to consider all the water bound to the protein as irrotationally bound.

In Table 1, the values of $\overline{R}^2$ for ellipsoidal geometry are bigger than those obtained employing spherical geometry. It means that the ellipsoidal geometry is the best option to describe PMR in HSA solutions and it is coherent with the reported geometry of this protein in solution [34, 35].

All the results showed and the analysis performed above suggest that the best model to describe PMR in HSA solutions, in our experimental conditions, is the 2SWEM considering an ellipsoidal geometry for the protein molecule. It is another option to describe PMR in protein solutions: to consider it not determined by a distribution of different types of water bound to the macromolecule as previously reported [18, 29], but to consider it determined by different correlation times for the rotation of the protein according to its geometry as previously recommended [23].

This result is particularly useful to update the physical model used to describe the relation between $\frac{1}{T_2}$ and η in blood plasma and blood serum samples [3, 5], which are specific medical applications based on PMR.

The approach used in this work only consider, for the bound water, the dipolar interaction between the two protons inside the water molecule, discarding other dipolar interactions such as those performed between: (i) two water protons belonging to different water molecules bounded to the protein, (ii) one proton belonging to one molecule of water bounded to the protein and another proton belonging to the macromolecular structure and (iii) one proton belonging to one molecule of water bounded to the protein and another proton belonging to the solvent. It is a limitation for both models used (2SWEM and 3SEM), decreasing its performances and reducing the capability of these models to estimate the physical parameters determined. It could be the case, for example, of τ_{R1} and τ_{R2}. To improve these results we suggest to use the 3 Tau model [39–41], which takes into account all this interaction. It is the subject of one undergoing work.

4 Conclusions

The 2 sites water exchange model considering ellipsoidal geometry is the best option to fit the ^{1}HMRD profiles in diluted HSA solutions, which allows to update the physical model previously presented to describe the theoretical dependence between the transverse proton magnetic relaxation rate and the protein dynamic viscosity in blood plasma and blood serum solutions. The physical parameters obtained from the fit, using this model, describe properly the diluted HSA solutions in comparison with previous experimental reports and theoretical estimations. This result can be

improved taking into consideration all the proton–proton dipolar interactions of the protons belonging to the bound water molecules.

Appendix

PMR in protein solutions is determined by the dominant contribution of the water protons [3, 19]. The other protons, belonging to the macromolecular structure, have magnetic relaxation times very short, much shorter than the magnetic relaxation times of the water protons at the protein solution and than the dead times of the majority of the equipments utilized to measure relaxation, then its contribution can be neglected. The physical model most commonly used to describe PMR in protein solutions is the 2SWEM [1, 3, 5, 6, 18–20, 22–25, 27],which considers two types of water: the water bound to the macromolecular surface and the free water. In this model the bound water is considered as irrotationally bound to the protein surface, such as $\tau_R \ll \tau_{res}^B (bound\ water\ residence\ time) \ll T_1, T_2$. Then, a fast exchange of water molecules between the bound and free water states will be established, and $R_1 = \frac{1}{T_1}$ can be calculated as follows [1, 3, 5, 6, 18–20, 22–25, 27]:

$$R_1 = P_{bulk} R_{1w}^{bulk} + P_B R_{1B} \tag{10}$$

In Eq. (10), R_{1B} represents the longitudinal proton magnetic relaxation rate of the protons belonging to the bound water molecules. P_{bulk} is the fraction of free water, such as $P_{bulk} + P_B = 1$. In this model the ^{1}H–^{1}H dipolar interaction inside the water molecule is defined as the main contribution to ^{1}H water relaxation. To evaluate R_{1w}^{bulk} and R_{1B} the following equation is considered [42–46]:

$$R_1(\omega_0) = \frac{9}{8}\left(\frac{\mu_0}{4\pi}\right)^2 \gamma^4 \left(\frac{h}{2\pi}\right)^2 \left[J_1(\omega_0) + J_2(2\omega_0)\right] \tag{11}$$

Equation (11) is obtained after computing the values of the probability for transitions between the Zeeman energy levels, as well as the temporal evolution of the population difference between these levels, and it is valid for the case of two dipolar interacting spin pairs $\left(I = \frac{1}{2}\right)$, where the dipolar interaction is modulated by the change of the angle between the vector joining the spin pair $(\vec{r})$ and the external and constant magnetic field $(\overrightarrow{B_0})$, remaining unchangeable the $|\vec{r}|$ [42, 47]. Here, h is the Planck's constant. The functions J_1 and J_2 are spectral density functions describing the water mobility inside the sample [47]:

$$J_i(\omega_0) = \int_{-\infty}^{\infty} K_i(\tau) e^{i\omega_0 \tau} d\tau \tag{12}$$

$$K_i(\tau) = \left(F_i(t) F_i^*(t+\tau)\right)_{AV} \tag{13}$$

where $K_i(\tau)$ is a correlation function, dependent of τ and independent of t, measuring the level of correlation of the system between its states at t and $t+\tau$. The values of i can be 1 and 2. $K_i(\tau)$ can be considered as a monoexponential function and Eq. (13) rewritten as [43]

$$K_i(\tau) = \left(F_i(t)F_i^*(t)\right)_{AV} e^{\frac{|\tau|}{\tau_C}} \tag{14}$$

In Eq. (14), τ_C is a constant of time measuring when the correlation between two states of the system reduces e (Euler) times. Then, Eq. (12) can be rewritten as follows [43]:

$$J_i(\omega_0) = \left(F_i(t)F_i^*(t)\right)_{AV} \frac{2\tau_C}{1+\left(\omega_0\tau_C\right)^2} \tag{15}$$

The functions F in Eqs. (13)–(15) are coordinate functions describing the relative positions of the two spin under dipolar interaction and, considering a fixed distance between the interacting protons ($\lfloor\vec{r}\rfloor = b$), then [47]:

$$\left(F_1(t)F_1^*(t)\right)_{AV} = \frac{2}{15b^6} \tag{16}$$

$$\left(F_2(t)F_2^*(t)\right)_{AV} = \frac{8}{15b^6} \tag{17}$$

Finally, combining Eqs. (11) and (15–17), it is possible to obtain:

$$R_1(\omega_0) = \frac{3}{10}\left(\frac{\mu_0}{4\pi}\right)^2 \frac{\gamma^4\left(\frac{h}{2\pi}\right)^2}{b^6}\left[\frac{\tau_C}{1+\left(\omega_0\tau_C\right)^2} + \frac{4\tau_C}{1+4\left(\omega_0\tau_C\right)^2}\right] \tag{18}$$

For the case of a water molecule irrotationally bound to the macromolecule, the movement modulating the dipolar interaction between the two protons inside the water molecule is the protein rotation. Then, $\tau_C = \tau_R$ and Eq. (18) can be rewritten as.

$$R_{1B}(\omega_0) = \frac{3}{10}\left(\frac{\mu_0}{4\pi}\right)^2 \frac{\gamma^4\left(\frac{h}{2\pi}\right)^2}{b^6}\left[\frac{\tau_R}{1+\left(\omega_0\tau_R\right)^2} + \frac{4\tau_R}{1+4\left(\omega_0\tau_R\right)^2}\right] \tag{19}$$

Even if you consider ^{1}H–^{1}H intermolecular dipolar interactions between protons located in different bound water molecules, or between one proton in a bound water molecule with another proton at the macromolecular structure, $\tau_C = \tau_R$. It is because, in spite of one should consider the exchange of water molecules between bound and bulk states as a process modulating the dipolar interaction ($\frac{1}{\tau_C} = \frac{1}{\tau_{res}^B} + \frac{1}{\tau_R}$) [26], $\tau_{res}^B \gg \tau_R$. Nevertheless, the model is focused in the intramolecular dipolar interaction between the protons inside the irrotationally bound water molecules,

which is a limitation. Another limitation is that this model does not take into consideration the dipolar interaction between water protons at the solvent and protons located in bound water molecules or in the protein structure, which is modulated by solvent water diffusion. Moreover, Eq. (19) does not consider interactions with unpaired electrons at the sample (dipolar, scalar and/or Curie interactions) [27, 48].

In Eq. (19), the values of $\tau_R \geq 10^{-9}s$ [1, 18, 19, 22–25] make R_{1B} a function of ω_0. For the case of the free water $\tau_C = 10^{-12}s - 10^{-11}s$ and R_1 is independent from ω_0, such as:

$$R_{1W}^{bulk} = \frac{3}{2}\left(\frac{\mu_0}{4\pi}\right)^2 \frac{\gamma^4\left(\frac{h}{2\pi}\right)^2 \tau_C}{b^6} \tag{20}$$

For the case of the bulk; the intermolecular ^{1}H–^{1}H dipolar interactions modulated by diffusion can be considered adding a term to Eq. (20), which is also ω_0 independent [43]. Combining Eqs. (10), (19) and (20), it is possible to obtain:

$$R_1(\omega_0) = R_{1w}^{\text{bulk}} + \delta_1\left[\frac{0.2\tau_R}{1+(\omega_0\tau_R)^2} + \frac{0.8\tau_R}{1+4(\omega_0\tau_R)^2}\right]$$

$$\delta_1 = P_b\frac{3}{2}\left(\frac{\mu_0}{4\pi}\right)^2\frac{\gamma^4\hbar^2}{b^6} \tag{21}$$

Despite Eq. (21) is the traditional model to describe PMR in protein solutions [1, 3, 6, 18, 19, 22–24, 27, 44], considering that usually the protein geometry is more near to one ellipsoid than to one sphere (mainly in solution) [32–35], the protein + water complex should be described using an ellipsoidal geometry and more than one correlation time.

If our dipolar interacting spin pairs (the protons inside the irrotationally bound water molecules) are assumed as included inside one rigid molecule with a geometry corresponding to a prolate ellipsoid ($a_1 > a_2 = a_3$, being a_1, a_2 and a_3 the lengths of the symmetry axes of the ellipsoid divided by 2) the spectral density functions can be described according to [45, 46]

$$J_i(\omega_0) = 2\left(F_i(t)F_i^*(t)\right)_{AV}\left[Q\left(\frac{\tau_{R1}}{1+(\omega_0\tau_{R1})^2}\right) + S\left(\frac{\tau_{R2}}{1+(\omega_0\tau_{R2})^2}\right) + U\left(\frac{\tau_{R3}}{1+(\omega_0\tau_{R3})^2}\right)\right] \tag{22}$$

Here, τ_{R1}, τ_{R2} and τ_{R3} are the correlation times for the rotation of the protein molecule around each symmetry axis of the ellipsoid. Q, S and U depend on the cosine of the angle between $\vec{r}$ and the main symmetry axis of the ellipsoid (l) [45, 46]:

$$Q = \frac{1}{4}\left(3l^2 - 1\right)^2 \tag{23}$$

$$S = 3l^2\left(1 - l^2\right) \tag{24}$$

$$U = \frac{3}{4}\left(l^2 - 1\right)^2 \tag{25}$$

The values of τ_{R1}, τ_{R2} and τ_{R3} can be related to the rotational diffusion coefficients for the movement around each axis of the ellipsoid (D_{R1}, D_{R2} and D_{R3}) as follows [45, 46]:

$$\frac{1}{\tau_{R1}} = 6D_{R2} \tag{26}$$

$$\frac{1}{\tau_{R2}} = 5D_{R2} + D_{R1} \tag{27}$$

$$\frac{1}{\tau_{R3}} = 2D_{R2} + 4D_{R1} \tag{28}$$

Combining Eqs. (16), (17) and (22)–(25), it is possible to obtain Eqs. (29), (30)and (31) for the cases in which the angle between $\vec{r}$ and the main symmetry axis of the ellipsoid takes values: 0, $\frac{\pi}{2}$ and $\frac{\pi}{4}$, respectively:

$$R_{1B}(\omega_0) = \frac{3}{10}\left(\frac{\mu_0}{4\pi}\right)^2 \frac{\gamma^4\left(\frac{h}{2\pi}\right)^2}{b^6}\left[\frac{\tau_{R1}}{1+\left(\omega_0\tau_{R1}\right)^2} + \frac{4\tau_{R1}}{1+4\left(\omega_0\tau_{R1}\right)^2}\right] \tag{29}$$

$$R_{1B}(\omega_0) = \frac{3}{10}\left(\frac{\mu_0}{4\pi}\right)^2 \frac{\gamma^4\left(\frac{h}{2\pi}\right)^2}{b^6}\left[\begin{array}{l} \frac{1}{4}\left(\frac{\tau_{R1}}{1+\left(\omega_0\tau_{R1}\right)^2} + \frac{4\tau_{R1}}{1+4\left(\omega_0\tau_{R1}\right)^2}\right)+ \\ \frac{3}{4}\left(\frac{\tau_{R3}}{1+\left(\omega_0\tau_{R3}\right)^2} + \frac{4\tau_{R3}}{1+4\left(\omega_0\tau_{R3}\right)^2}\right) \end{array}\right] \tag{30}$$

$$\begin{aligned} R_{1B}(\omega_0) = \frac{3}{10}\left(\frac{\mu_0}{4\pi}\right)^2 \frac{\gamma^4\left(\frac{h}{2\pi}\right)^2}{b^6}\Bigg[&\frac{1}{16}\left(\frac{\tau_{R1}}{1+\left(\omega_0\tau_{R1}\right)^2} + \frac{4\tau_{R1}}{1+4\left(\omega_0\tau_{R1}\right)^2}\right) \\ &+\frac{12}{16}\left(\frac{\tau_{R2}}{1+\left(\omega_0\tau_{R2}\right)^2} + \frac{4\tau_{R2}}{1+4\left(\omega_0\tau_{R2}\right)^2}\right)+\frac{3}{16}\left(\frac{\tau_{R3}}{1+\left(\omega_0\tau_{R3}\right)^2} + \frac{4\tau_{R3}}{1+4\left(\omega_0\tau_{R3}\right)^2}\right)\Bigg] \end{aligned} \tag{31}$$

According to Eqs. (29)–(31), a general case (including all possible angles between $\vec{r}$ and the main symmetry axis of the ellipsoid) will be:

$$R_{1B}(\omega_0) = \frac{3}{10}\left(\frac{\mu_0}{4\pi}\right)^2 \frac{\gamma^4\left(\frac{h}{2\pi}\right)^2}{b^6}\left[\sum_{i=1}^{3} Z_i\left(\frac{\tau_{Ri}}{1+\left(\omega_0\tau_{Ri}\right)^2} + \frac{4\tau_{Ri}}{1+4\left(\omega_0\tau_{Ri}\right)^2}\right)\right] \tag{32}$$

where Z_i are constants resulting of the sum of all terms containing to $\left(\frac{\tau_{Ri}}{1+\left(\omega_0\tau_{Ri}\right)^2} + \frac{4\tau_{Ri}}{1+4\left(\omega_0\tau_{Ri}\right)^2}\right)$. Combining Eqs. (10) and (32) it is possible to obtain:

$$R_1(\omega_0) = R_{1w}^{bulk} + \delta_1 \left[\sum_{i=1}^{3} Z_i \left(\frac{0.2\tau_{Ri}}{1 + (\omega_0 \tau_{Ri})^2} + \frac{0.8\tau_{Ri}}{1 + 4(\omega_0 \tau_{Ri})^2} \right) \right]$$

$$\delta_1 = P_b \frac{3}{2} \left(\frac{\mu_0}{4\pi} \right)^2 \frac{\gamma^4 \hbar^2}{b^6} \tag{33}$$

A prolate ellipsoid has only two rotational correlation times due to: the rotation around one axis parallel to its main symmetry axis and another rotation around one axis perpendicular to its main symmetry axis [38]. Then, in Eq. (33), we can consider that $\tau_{R2} = \tau_{R3}$ $(a_2 = a_3)$ and this equation can be rewritten as follows:

$$R_1(\omega_0) = R_{1w}^{bulk} + \left[\sum_{i=1}^{2} \beta_i \left(\frac{0.2\tau_{Ri}}{1 + (\omega_0 \tau_{Ri})^2} + \frac{0.8\tau_{Ri}}{1 + 4(\omega_0 \tau_{Ri})^2} \right) \right] \tag{34}$$

In Eq. (34), $\beta_1 = \delta_1 Z_1$ and $\beta_2 = \delta_1 (Z_2 + Z_3)$. Please, note that the number 5 has been extracted from the bracket as a common factor. R_{1W}^{bulk} has not been detailed as in Eq. (20) due to its independence with ω_0. On the other hand, $P_{bulk} \approx 1$ without losing rigor [3, 5, 6, 18, 19].

Acknowledgements The authors want to thanks to the researchers of the NMR laboratory at the University of MONS in Belgium for the collaboration and treatment during the experiment. Moreover, we appreciate the support received from the Universidad Autónoma de Santo Domingo (UASD) and its authorities to develop this work.

Authors' contribution Conceptualization: Manuel Arsenio Lores Guevara, Carlos Alberto Cabal Mirabal; Methodology: Manuel Arsenio Lores Guevara, Sophie Laurent, Robert N. Müller; Formal analysis and investigation: Manuel Arsenio Lores Guevara, Néstor Juan Rodríguez de la Cruz, Yasser Rodríguez de la Cruz; Writing-original draft preparation: Manuel Arsenio Lores Guevara, Néstor Juan Rodríguez de la Cruz; Writing-review and editing: Manuel Arsenio Lores Guevara, Juan Carlos García Naranjo, Néstor Juan Rodríguez De la Cruz, Sophie laurent, Robert N. Müller, Carlos Alberto Cabal Mirabal, Fabián Tamayo Delgado; Supervision: Manuel Arsenio Lores Guevara.

Funding This work was supported by the FNRS (FONDS NATIONAL DE LA RECHERCHÉ SCIENTIFIQUE) from Belgium.

Data availability No datasets were generated or analysed during the current study.

Declarations

Conflict of interests The authors declare no competing interests.

Ethical approval Not applicable.

References

1. M.A. Lores-Guevara, J.C. García-Naranjo, C.A. Cabal-Mirabal, Appl. Magn. Reson. **A50**, 541 (2019). https://doi.org/10.1007/s00723-018-1104-0

2. C.A. Cabal-Mirabal, A. Fernández-García, M.A. Lores-Guevara, E. González-Dalmau, L. Oramas-Díaz, Appl. Magn. Reson. **A49**, 589 (2018). https://doi.org/10.1007/s00723-018-0985-2
3. Y. Mengana-Torres, M.A. Lores-Guevara, H. Ferrales-Milán, L.C. Suárez-Beyries, S.J. Rosales-Rodríguez, I. Rodríguez-Reyes, J.C. García-Naranjo, Y. Alonso-Geli, Appl. Magn. Reson. **A55**, 527 (2024). https://doi.org/10.1007/s00723-024-01644-0
4. Y. Mengana-Torres, M.A. Lores-Guevara, J.C. García-Naranjo, B.T. Ricardo-Ferro, L.C. Suárez-Beyries, I.C. Rodríguez-Reyes, J. Phillippé, Int. J. Biochem. Biophys. Mol. Biol. **A4**, 25 (2019) https://doi.org/10.11648/j.ijbbmb.20190402.12
5. M.A. Lores-Guevara, Y. Mengana-Torres, J.C. García-Naranjo, N. Rodríguez-Suárez, L.C. Suárez-Beyries, M.A. Marichal-Feliú, T. Simón-Boada, I.C. Rodríguez-Reyes, J. Phillippé, Appl. Magn. Reson. **A49**, 1075 (2018). https://doi.org/10.1007/s00723-018-1026-x
6. N.J. Rodríguez-De la Cruz, Y. Mengana-Torres, J.C. García-Naranjo, B.T. Ricardo-Ferro, Y. Alonso-Geli, E. Guerrero-Piña, Y. Araujo-Durán, L.C. Suárez-Beyries, I. Rodríguez-Reyes, S.J. Rosales-Rodríguez, M. Guevara, Hemoglobin. **A49**, 172 (2025) https://doi.org/10.1080/03630269.2025.2493949
7. M.A. Lores-Guevara, C.A. Cabal-Mirabal, A. Fernández-García, Y. Mengana-Torres, J.C. García-Naranjo, I. Rodríguez-Reyes, L.C. Suárez-Beyríes, S.J. Rosales-Rodríguez, Y. Alonso-Geli, An. Acad. Cienc. Cuba. **A15** (2025)
8. Y. Mengana-Torres, M.A. Lores-Guevara, Y. Alonso-Geli, L.C. Suárez-Beyríes. N. Rodríguez-Suárez, Rev. Cuba. Quím. **A36**, 1 (2024)
9. L. Gravitz, S. Pincock, Nature **A515**, S1 (2014). https://doi.org/10.1038/515S1a
10. F.B. Piel, M.H. Steinberg, D.C. Rees, N. Engl, J. Med. **A376**, 1561 (2017). https://doi.org/10.1056/NEJMra1510865
11. E.A. Ajjack, H.A. Awooda, S.E. Adalla, Int. J. Hematol. Disord. **A1**, 8 (2014) https://doi.org/10.12691/ijhd-1-1-2
12. L.V. Parise, N. Berliner, Blood (2016). https://doi.org/10.1182/blood-2015-12-674606
13. E.I. Obeagu, K.C. Ochei, B.N. Nwachukwu, B.O. Nchuma, Sch. J. App. Med. Sci. **A3**, 2244 (2015)
14. A. Nowogrodzki, Nature **A596**, S13 (2021). https://doi.org/10.1038/d41586-021-02143-z
15. L.M. Somoano, M.A. Lores-Guevara, J.C. García-Naranjo, J.E. Niesor, A. Perez, I. Rodríguez, S. Rosales, F. Tamayo-Delgado, Res. Biomed. Eng. **A38**, 831 (2022) https://doi.org/10.1007/s42600-022-00224-0
16. N. Archer, F. Galacteros, C. Brugnara, Am. J. Hematol. **A90**, 934 (2015). https://doi.org/10.1002/ajh.24116
17. L. Somoano-Delgado, F. Tamayo-Delgado, C.C. García-Cruz, A.T. Suárez-Olivares, D.E. Monet-Alvarez, A. Salabert-Revilla, H. Cruz-Vadell, L.C. Suárez-Beyries, Y. Araujo-Durán, Y. Alonso-Geli, M.A. Lores-Guevara, *Proceedings of the 21th International Conference and School on Magnetic Resonance and its applications*, Saint-Petersburg, 2024, p. 123
18. M.A. Lores-Guevara, C.A. Cabal-Mirabal, R.N. Müller, S. Laurent, F. Tamayo-Delgado, J.C. García-Naranjo, Appl. Magn. Reson. **A53**, 387 (2022). https://doi.org/10.1007/s00723-021-01452-w
19. M.A. Lores-Guevara, C.A. Cabal-Mirabal, Appl. Magn. Reson. **A28**, 79 (2005). https://doi.org/10.1007/BF03166995
20. Y. Cabrales, M.A. Lores-Guevara, Y. Machado, Appl. Magn. Reson. **A33**, 207 (2008). https://doi.org/10.1007/s00723-008-0074-z
21. N.J. Rodríguez-De la Cruz, M.A. Lores-Guevara, C.A. Cabal-Mirabal, R.N. Müller, S. Laurent, F. Tamayo-Delgado, J.C. García-Naranjo, *Proceedings of the 21th International Conference and School on Magnetic Resonance and its applications*, Saint-Petersburg, 2024, p. 125
22. O.K. Dazkiewic, J.W. Hennel, B. Lubas, T.W. Szczepkowski, Nature **A200**, 1006 (1963). https://doi.org/10.1038/2001006a0
23. S.H. Koenig, W.E. Schillinger, J. Biol. Chem. **A244**, 3283 (1969)
24. T.R. Lindstrom, S.H. Koenig, J. Magn. Reson. **A15**, 344 (1974)
25. S. Kiihne, R.G. Bryant, Biophys. J. **A78**, 2163 (2000) https://doi.org/10.1016/S0006-3495(00)76763-4
26. B. Halle, Phil. Trans. R. Soc. Lond. B. **A359**, 1207 (2004) https://doi.org/10.1098/rstb.2004.1499
27. S.H. Koenig, W.E. Schillinger, J. Biol. Chem. **A244**, 6520 (1969)
28. K. Hallenga, S.H. Koenig, Biochemistry **A15**, 4255 (1976)
29. K. Venu, V.P. Denisov, B. Halle, J. Am. Chem. Soc. **A119**, 3122 (1997) https://doi.org/10.1021/ja963611t

30. B. Halle, H. Johannesson, K. Venu, J. Magnet. Reson. **A135**, 1 (1998) https://doi.org/10.1006/JMRE.1998.1534
31. B.C. Thompson, M.R. Waterman, G.L. Cottam, Arch. Biochem. Biophys. **A166**, 193 (1975)
32. M.A. Kiselev, I.A. Gryzunov, G.E. Dobretsov, M.N. Komarova, Biofizika **A46**, 423 (2001)
33. Y.X. Huang, Z.J. Wu, B.T. Huang, M. Luo, PLoS One. **A8**, e81708 (2013) https://doi.org/10.1371/journal.pone.0081708
34. K. Monkos, Biochimica et Biophysica Acta (BBA) **1700**(1), 27 (2004)
35. M.L. Ferrer, R. Duchowicz, B. Carrasco, J.´ García, A. De la Torre, U. Acuna, Biophys. J. **A80**, 2422 (2001)
36. B. Halle, T. Andersson, S. Forsen, B. Lindman, J. Am. Chem. Soc. **A103**, 500 (1981)
37. M.A. Lores-Guevara, C.A. Cabal-Mirabal, O. Nascimento, A.M. Gennaro, Appl. Magn. Reson. **A30**, 121 (2006). https://doi.org/10.1007/BF03166986
38. Z.H. Endre, P.W. Kuchel, Biophys. Chem. **A24**, 333 (1986). https://doi.org/10.1016/0301-4622(86)85039-6
39. D.A. Faux, P.J. McDonald, N.C. Howlett, Phys. Rev. E. **A95**, (2017) https://doi.org/10.1103/PhysRevE.95.033116.
40. D.A. Faux, P.J. McDonald, Phys. Rev. E. **A95**, (2017) https://doi.org/10.1103/PhysRevE.95.033117.
41. D.A. Faux, P.J. McDonald, Phys. Rev. E. **A98**, (2018) https://doi.org/10.1103/PhysRevE.98.063110.
42. I. Solomon, Phys. Rev. **A99**, 559 (1955)
43. N. Bloembergen, E.M. PurceH, R.V. Pound, Phys. Rev. **A73**, 679 (1948)
44. C.A. Cabal- Mirabal, M.A. Lores-Guevara, V.I. Chizhik, S.O. Rabdano, J.C. García-Naranjo, Appl. Magn. Reson. (2020). https://doi.org/10.1007/s00723-020-01241-x
45. D.E. Woessner, J. Chem. Phys. **A37**, 647 (1962)
46. D.E. Woessner, B.S. Snowden Jr., G.H. Meyer, J. Chem. Phys. **A50**, 719 (1969)
47. J.R. Kubo, K. Tomita, Phys. Soc. Japan **A9**, 888 (1954)
48. P.S. Hubbard, Revs. Modern Phys. **A33**, 249 (1961)

Authors and Affiliations

Néstor Juan Rodríguez de la Cruz[1] · Carlos Alberto Cabal Mirabal[2,3] · Robert N. Müller[4] · Sophie Laurent[4] · Fabian Tamayo Delgado[2] · Juan Carlos García Naranjo[2] · Yasser Rodríguez de la Cruz[1] · Manuel Arsenio Lores Guevara[2,3]

✉ Manuel Arsenio Lores Guevara
manuellores2@gmail.com

[1] Escuela de Física, Facultad de Ciencias, Universidad Autónoma de Santo Domingo, Zona Universitaria, Distrito Nacional, Santo Domingo, República Dominicana

[2] Centro de Biofísica Médica, Universidad de Oriente, Patricio Lumumba S/N, CP: 90500 Santiago de Cuba, Cuba

[3] Centro de Neurociencias de Cuba, La Habana, Cuba

[4] Laboratoire de RMN Et d'Imagerie Moléculaire, Service de Chimie Générale, Organique Et Biomédicale, Faculté de Médecine Et de Pharmacie, Université de Mons, Mons, Belgique